Full Paper

CHARACTERISATION OF LIQUATION PRODUCTS IN A NICKEL BASE SUPERALLOY

K.M. Oluwasegun
Department of Metallurgy and Materials, University of Birmingham, B15 2TT, United Kingdom

M.O. Adeoye
Department of Materials Science and Engineering Obafemi Awolowo University, Ile-Ife.
madeoye@oauife.edu.ng

P.O. Atanda
Department of Materials Science and Engineering Obafemi Awolowo University, Ile-Ife.

O.E. Olorunniwo
Department of Materials Science and Engineering Obafemi Awolowo University, Ile-Ife.

B. Aremo
Centre for Energy Research and Development, Obafemi Awolowo University, Ile-Ife.

ABSTRACT

In this communication, detailed micro structural examination has been made on the dissolution behavior of the γ' strengthening precipitates in the heat affected zone (HAZ) during a solid state welding process of a powder metallurgy (PM) nickel based superalloy. The HAZ microstructures of this nickel based superalloy were simulated using Gleeble thermomechanical simulation system. The microstructural examination of the simulated HAZs shows that the large sized γ' precipitates (~0.8–3μm) survived their solvus temperature during the welding simulation to temperatures where they are thermodynamically favourable to react with the surrounding γ matrix, resulting in localized melting of the precipitates below the alloy's solidus and concomitant formation of eutectic liquid film by a eutectic type reaction. Microanalysis and electron diffraction were used to study the liquation products. The results are used to derive the origin of the liquation during the solid state welding of the alloy.

Keywords: *Superalloy, nickel, Electron microscopy, Heat-affected zones*

1. INTRODUCTION

Liquation cracking is a prominent problem that is encountered during conventional welding of precipitation hardened alloys (Pepe and Savage, 1967; Prager and Shira, 1968; Kelly, 1990; Henderson *et al.* 2004; Wang *et al.*, 2005; Unfried *et al.*, 2009). The heat affected zone (HAZ) hot cracking during various fusion welding of nickel based superalloy has been majorly related to the constitutional liquation of γ' precipitates (Lin *et al.* 1993; Ojo and Chaturvedi, 2005; Ola *et al.*, 2010). This has led to the use of supposedly exclusive solid state friction joining processes. However, the dissolution behaviour of γ' precipitates during solid state welding and the nature of the product formed have not yet been reported in the literature, and this needs to be understood for optimal weld properties.

This research on the dissolution behaviour of γ' precipitates during solid state welding has been carried out in response to the unrelenting drive towards increasing the overall efficiency of gas turbines in modern aircraft engines and power generation systems by the production/welding of jet engines that will burn fuel more effectively at higher temperatures, and thus enhancing global demand for the reduction of emission

Both transmission electron microscopy (TEM) and scanning electron microscopy (SEM) have been used to understand the dissolution behaviour of the strengthening precipitates during the solid state welding of a powder metallurgy (PM) nickel based superalloy and also determine the crystallographic nature of the constitutional liquation products observed after the rapid heating of welding.

2. EXPERIMENTAL PROCEDURES

The material used in this work is a new generation nickel base superalloy, developed by Rolls Royce Plc having the following chemical composition (wt%): 15Cr, 18.5Co, 5Mo, 3Al, 3.6Ti, 2Ta, 0.5Hf, 0.015B, 0.06Zr, 0.027C balance nickel. The base alloy has been standard solution heat treated at 1120°C for 4hours and aged at 760°C for 8 hours with subsequent air cooling. The as-received inertial friction welds of this alloy were sliced to dimensions 20 mm × 12 mm × 10 mm. The heat affected zones were simulated by a Gleeble thermo-mechanical simulation system. Cylindrical specimens of 8mm diameter and 7.96mm length were prepared from the base alloy, RR1000, heated to 1150, 1175, 1200 and 1225°C at a rate of 20°C/s and held for 1 s at all temperatures followed by water quenching. Condition close to equilibrium (at a slow heating rate 5°C/min, holding for 1 h) was also simulated at the above specified temperatures. Samples were polished using standard metallographic techniques and were subsequently electrolytically etched in 10% orthophosphoric acid solution at 3.5 V for 3s. TEM samples were

prepared by twin jet electro polishing and a Quanta 3D FEGSEM FIB equipped with gallium focussed ion beam. Phase examination and characterisation were carried out on an FEI-XL30 SEM and an FEI Tecnai F20 TEM.

3. Results And Discussion

3.1. Microstructures of the base alloy

Phase quantification of the solution heat treated base PM alloy using optical, scanning and transmission electron microscopy in conjunction with image J analysing software showed precipitation of ~48 vol.% ordered intermetallic phase within the grain and at the grain boundaries of the γ matrix. They consisted of a fairly regular distribution of primary cuboidal γ', 0.8 – 3 μm in size, fine (100-500 nm) spheroidal secondary γ' and very fine tertiary γ' (5-30 nm) (Fig.1a-c). Super lattice reflections from selected area diffraction pattern (SADP) from a region of both γ' and γ at different zone axes confirmed them to be coherent with the disordered fcc γ matrix (a=3.59 Å) with a cube-cube orientation relationship (Fig.2).

3.2. Microstructures of the as-welded HAZs

Figure 3 shows the microstructural evolution between the bond line zone (BLZ) and the HAZ. These variations in the microstructures suggest thermal gradient across the weld region. The dissolution behaviour of the main strengthening phase, γ' as observed within 300 μm of the weld and the nature of the product formed have been investigated and presented in the following sections.

3.3. Microstructures of the simulated/quenched HAZs

The simulated HAZ microstructure of a sample rapidly heated to 1150°C at 20°C/s and water quenched showed that the intragranular secondary γ' precipitates dissolved completely and re-precipitated as very fine γ' while the primary γ' particles appeared not to be affected (Fig. 4a). However, in samples heated to 1175°C, primary γ' particles appeared to have survived their solvus temperature (~1160°C), but constitutionally liquated (Fig. 4b) with re-solidification features observed at the γ–γ' interface. On increasing the simulation temperature to 1200°C and 1225°C complete liquation of the intergranular and transgranulay primary γ' particles were observed (Fig. 4c). These precipitates were observed to dissolve without liquation under equilibrium condition of 5oC/min heating rate and holding time of 1hr at each temperature with subsequent air cooling (Fig. 5).

3.4. γ' dissolution behavior during rapid heating

Figure 6 shows SEM images of two liquating transgranular primary γ' precipitates. These micrographs illustrate how the precipitates shrink and form a eutectic-like product at the γ/γ' interface. The departure from equilibrium structure as a result of rapid heating could have led to the re-distribution of solute elements as the system would be striving to maintain equilibrium, resulting in the precipitate shrinking from its original size to a smaller size (Cam and Kocak, 1998). SEM and TEM EDX line scans show that the liquation product has an intermediate composition of γ and γ' solute elements (Fig.7). This was further confirmed by TEM SADPs taken from the liquation product along different zone axes (Fig. 8). Bright diffraction spots from the SADPs are the common reflections from both γ and γ'. Figures 6, 7 and 8 therefore suggest that the dissociation and thus the shrinking of primary γ' particles during rapid heating coupled with the dissolution of secondary and tertiary

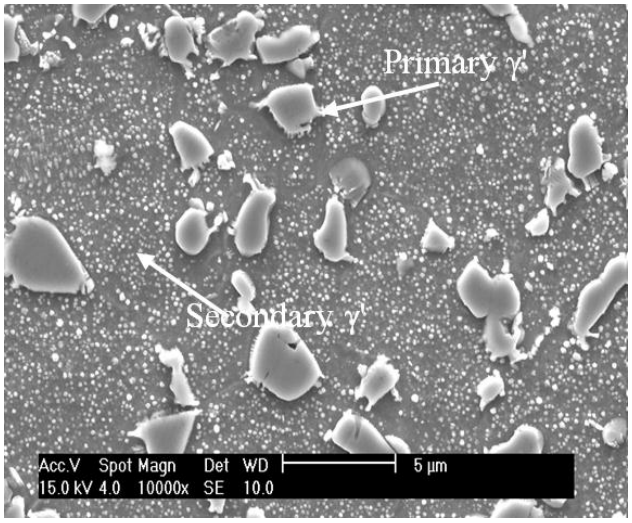

(a)

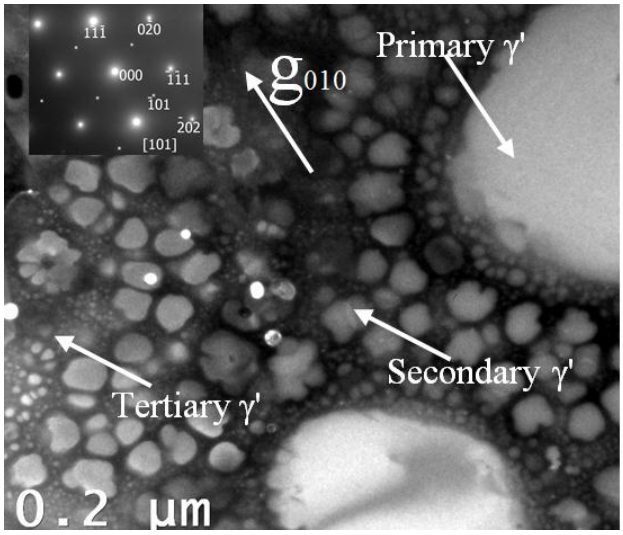

(b)

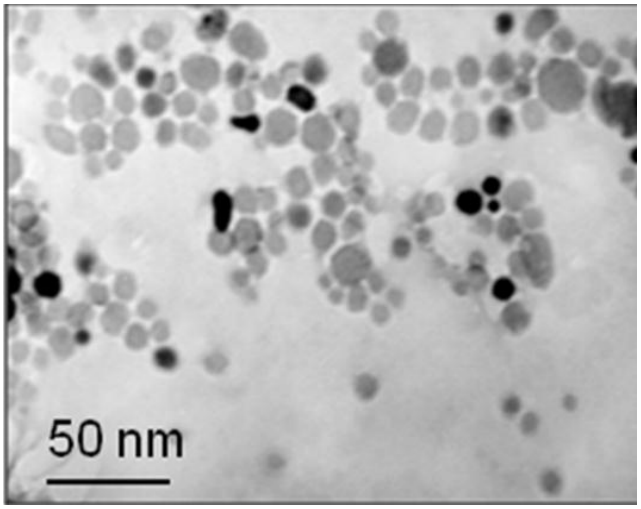

Figure 1: (a) SEM images of primary and secondary γ' respectively (b) TEM dark field (DF) image of the trimodal γ' precipitates (c) Tertiary γ' extracted by carbon replica (the dark tertiary γ' may be due to etching effect)

γ' in the vicinity of the shrinking primary γ', enriches the γ/γ' interface with solute atoms until an equilibrium condition is reached where it is thermodynamically favourable for a localized melting to occur within the eutectic temperature range of the alloy at the γ/γ' interface.

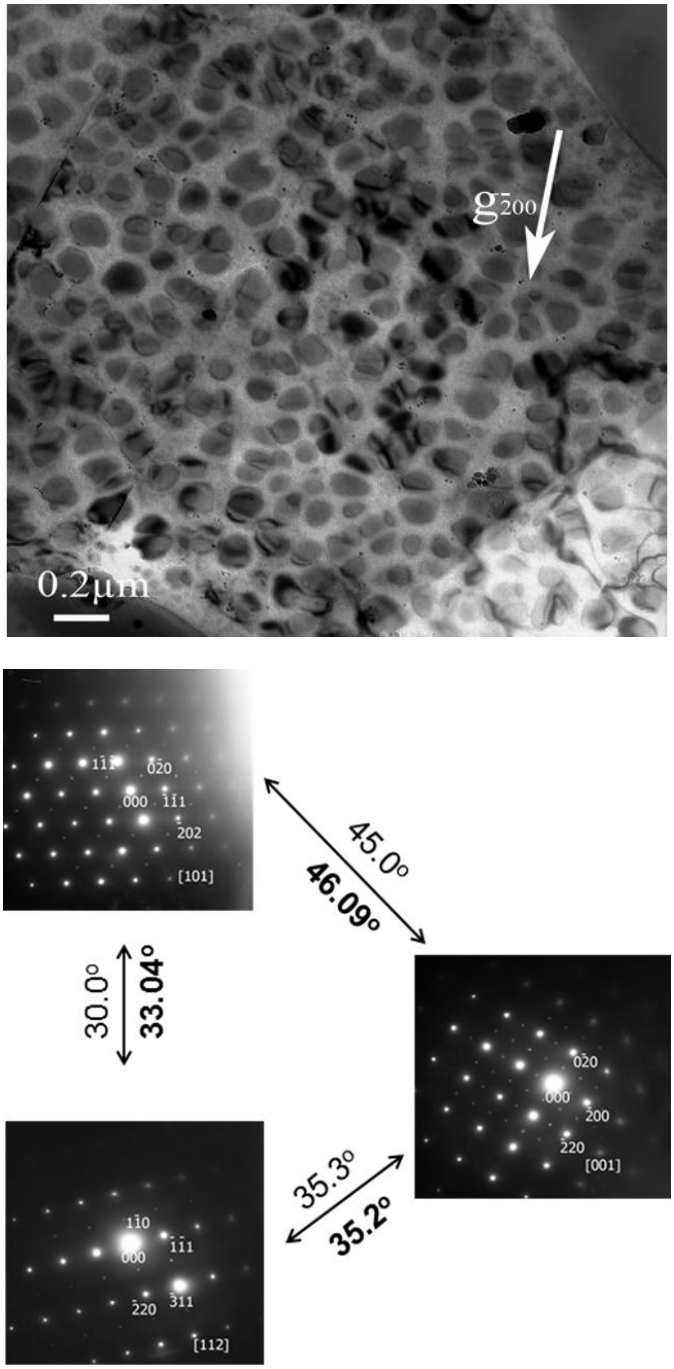

*Figure 2: (a) TEM DF image along [001] zone axis showing intragranular γ' precipitate within the γ matrix (b) Composite SADPs from both γ and γ', showing superlative reflections from the ordered γ' coherent with the disordered γ matrix with a cube-cube orientation relationship. The **bold** angles are the measured total tilt angle while the unbold are the calculated angles.*

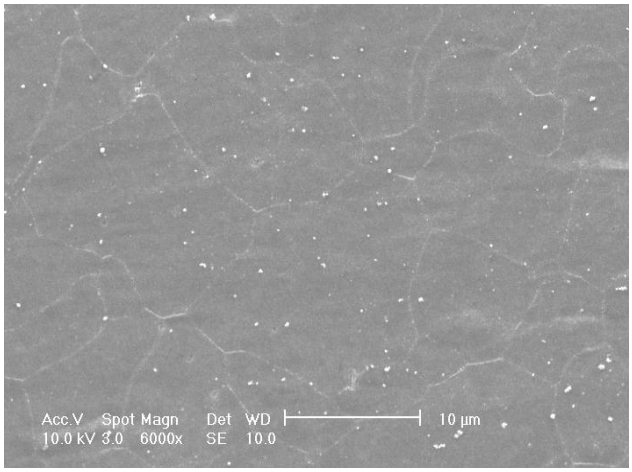

(a)

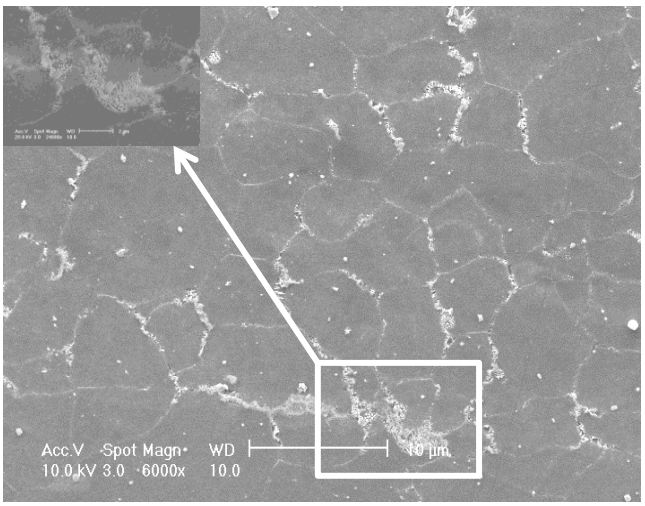

(b)

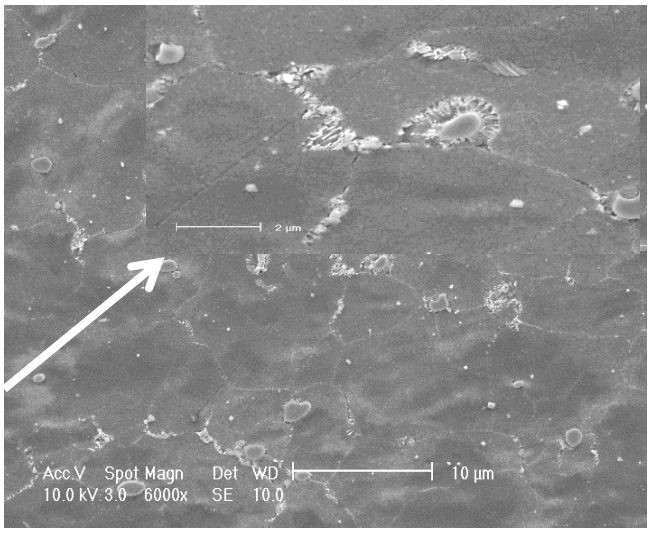

(c)

Figure 3: SEM images showing microstructural evolution at (a) BLZ (b) HAZ where complete primary γ' liquation occurs (c) HAZ where incomplete liquation of transgranular primary γ' occurs in as-welded sample.

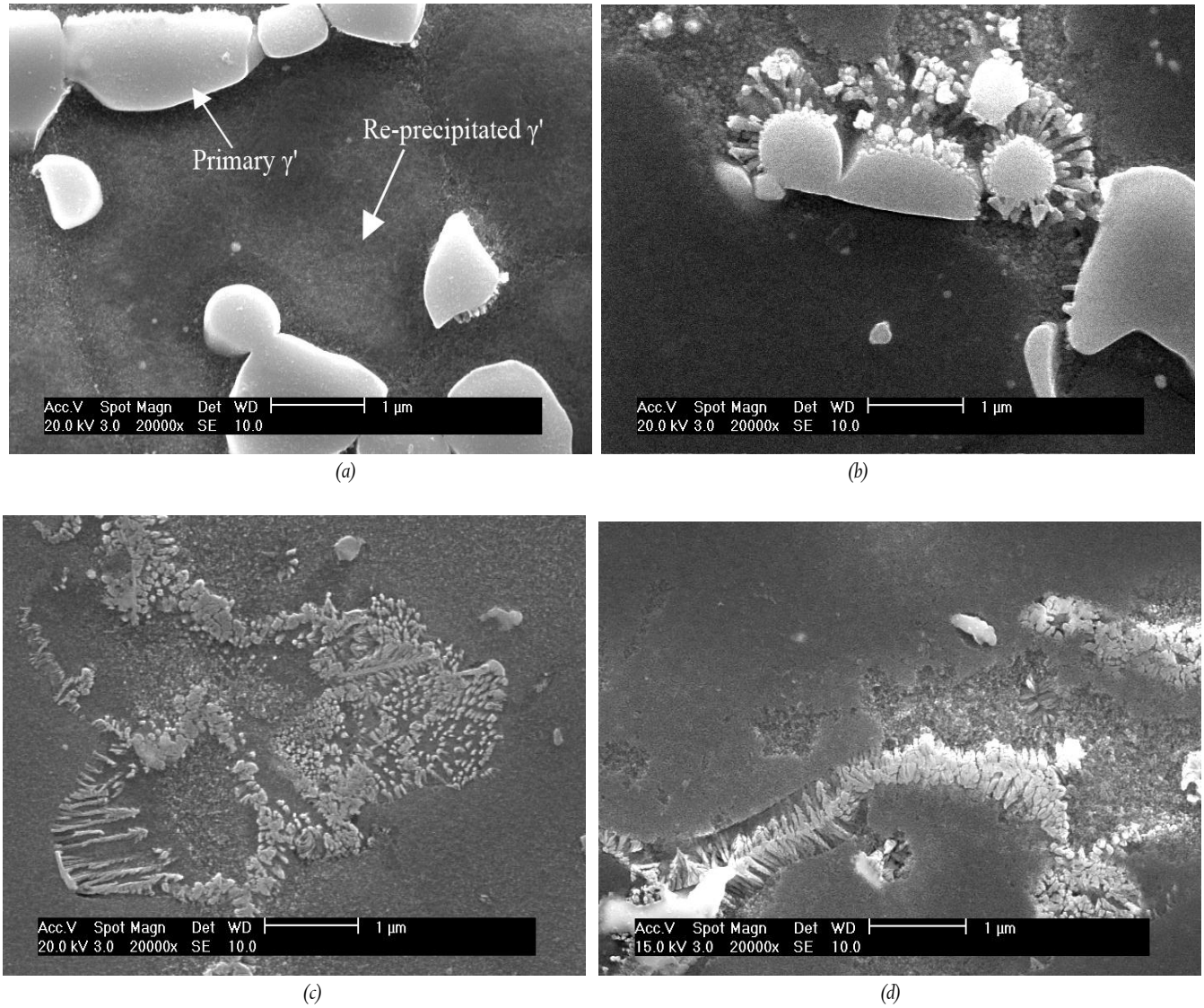

(a) *(b)*

(c) *(d)*

Figure 4: Simulated HAZ microstructure in a sample rapidly heated (20oC/s) to (a) 1150oC (b) 1175oC (c) 1200oC (d) 1225oC

The formation of constitutional liquid during solid state welding could have an attendant effect on the strength of the weld. According to the model proposed by Miller and Chadwick (1967), the minimum tensile stress, σ required to cause grain boundary decohesion is given as:

$$\sigma = 2\gamma/h \quad (1)$$

Where γ is the surface tension on a boundary containing liquid film of thickness h. This implies that the infiltration of the constitutional liquid along grain boundaries will lower solid-solid cohesive strength of the alloy during welding.

4. CONCLUSION

Rapid heating during inertia friction welding, a nominal solid state welding has been found to enhance constitutional liquation of primary γ' precipitates. The re-solidified liquation product formed has been identified as a eutectic of γ and γ' phases. The occurrence of constitutional liquid during a nominal solid state welding process could have an attendant effect on the strength of the weld by wetting and infiltrating grain boundaries and thus enhancing their decohesion.

REFERENCES

Cam, G. and M. Kocak, *Progress in joining of advanced materials.* International Materials Reviews, 43(1): p. 1-44, 1998.

Henderson, M.B., D. Arrell, M. Larsson, G. Marchant, *Nickel based superalloy welding practices for industrial gas turbine applications.* Science and Technology of Welding and Joining, 9(1): 13-21, 2004.

Kelly, T.J., *Welding metallurgy of investment cast nickel-based superalloys* Weldability of Materials, 151-157, 1990.

Lin, W., J.C. Lippold, and W.A. Baeslack, *An evaluation of heat-affected zone liquation cracking susceptibility.1. Development of a method for quantification.* Welding Journal, 72: S135-S153. 1993.

Miller, W.A. and G.A. Chadwick, On magnitude of solid/liquid interfacial energy of pure metals and its relation to grain boundary melting. Acta Metallurgica, 15: 607-614, 1967.

1115-9782 © 2011 Ife Journal of Technology

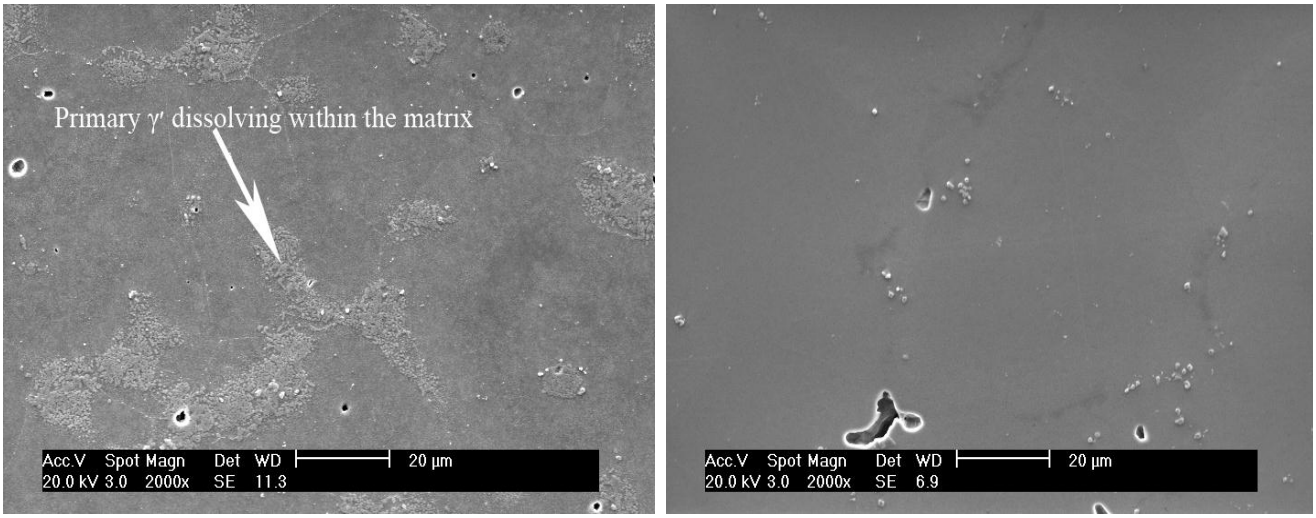

(a) (b)

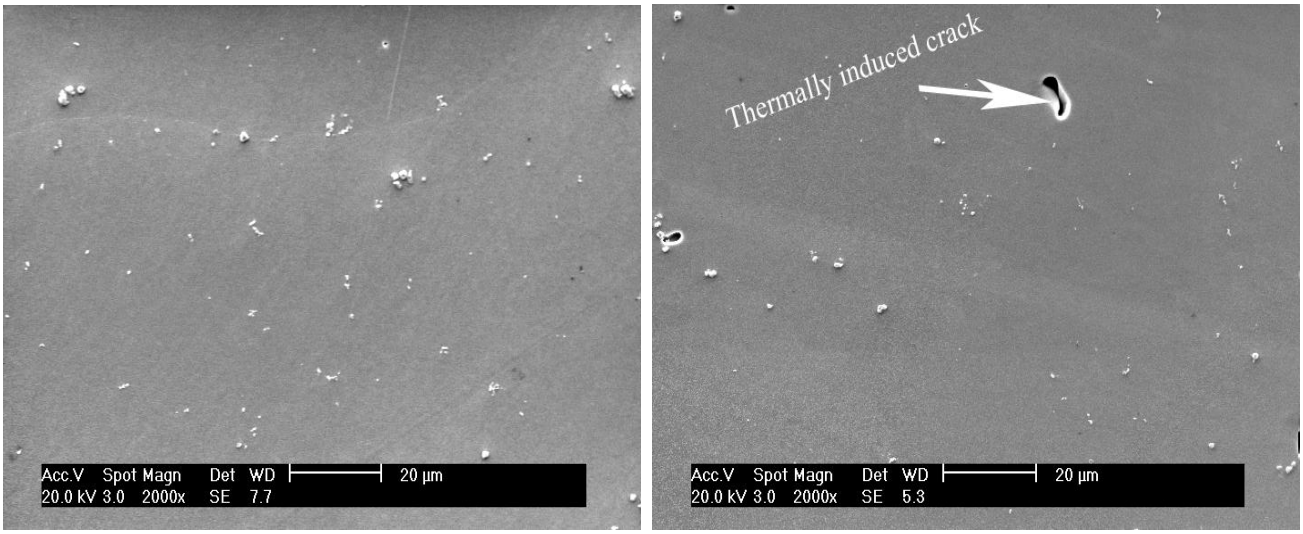

(c) (d)

Figure 5: SEM micrographs of γ' dissolution under equilibrium condition (5oC/min) to (a) 1150oC (b) 1175oC (c) 1200oC (d) 1225oC

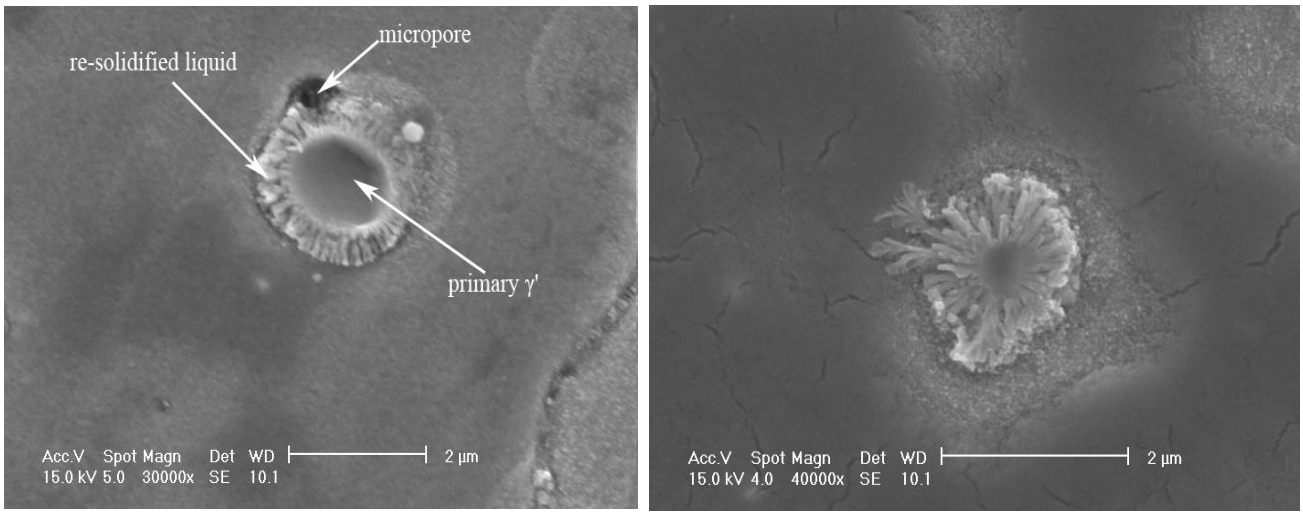

(a) (b)

Figure 6: (a,b) SEM micrographs showing how liquating primary γ' shrinks within the matrix during rapid heating.

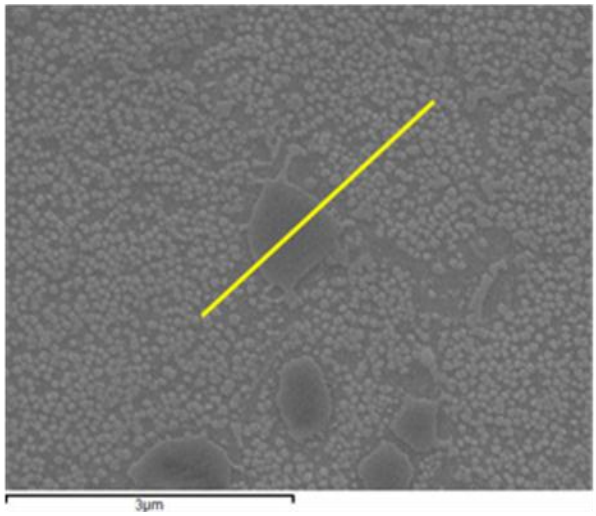

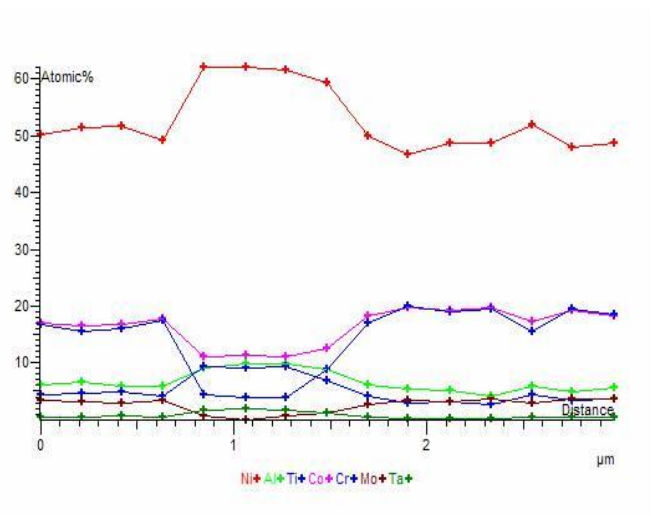

(a)

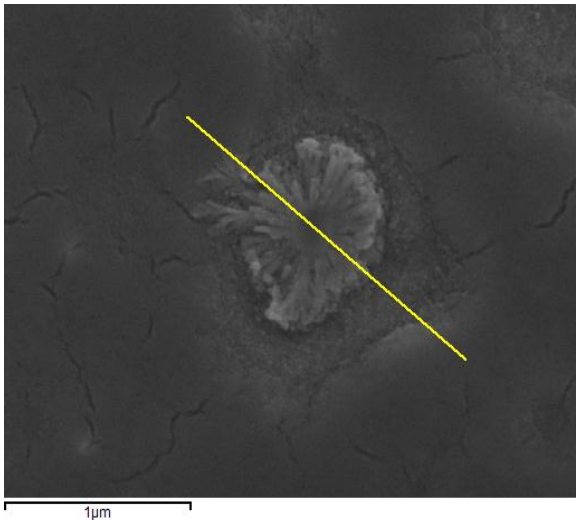

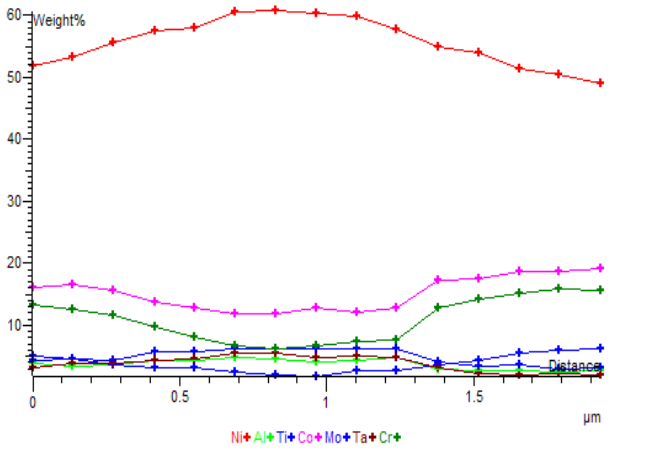

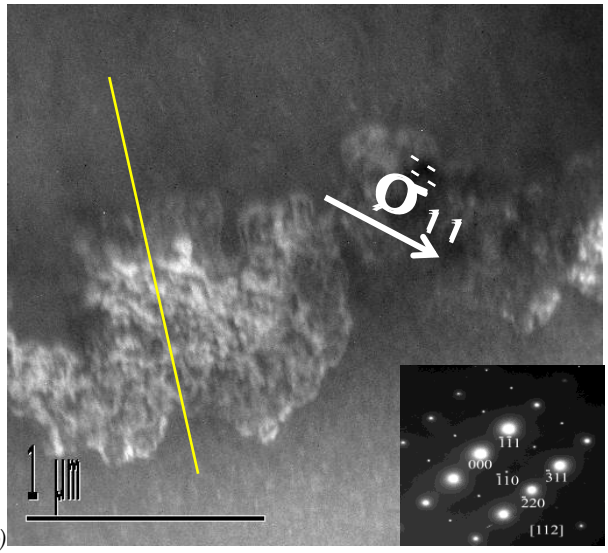

(b)

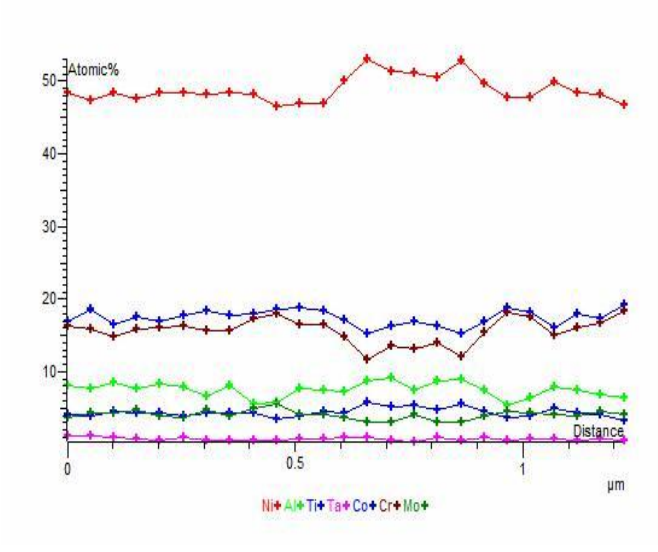

(c)

Figure 7: SEM micrographs and EDX line scans across (a) primary γ' in base alloy and an EDX line scans across the precipitate (b) liquated primary γ' with the EDX line scan (c) TEM DF image of a γ-γ' eutectic product taken along [112] zone axis and an EDX line scans across the eutectic product.

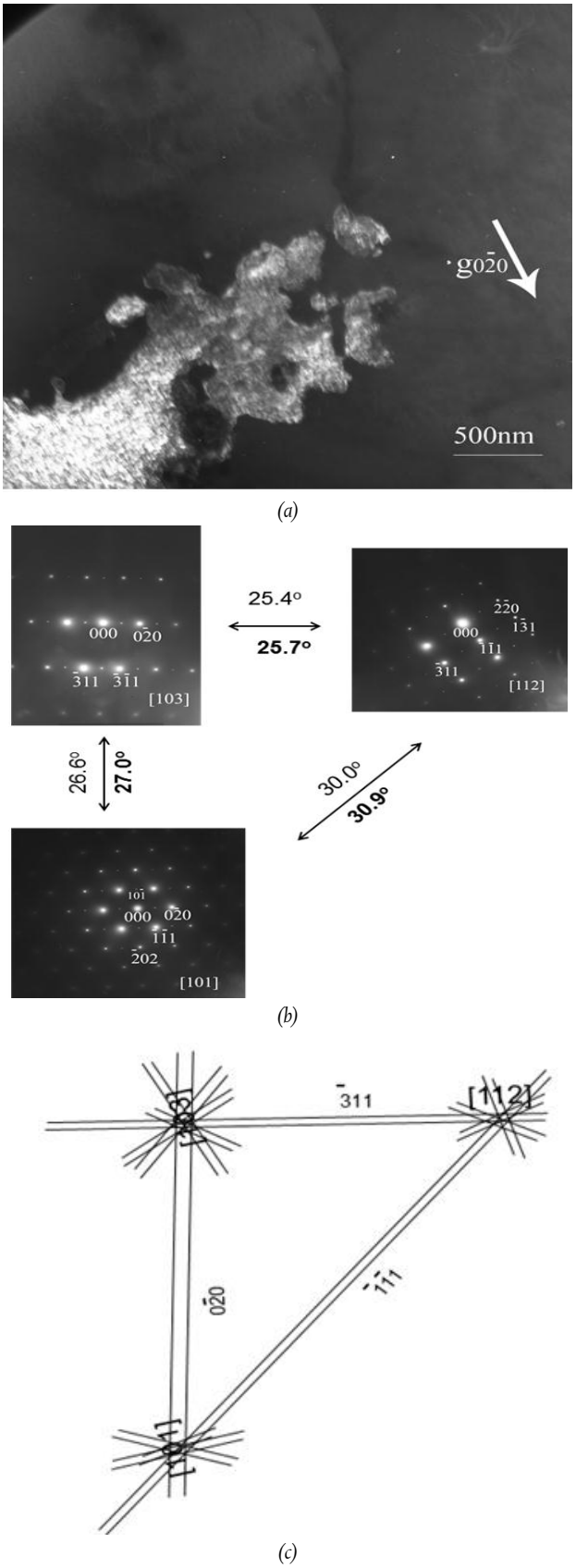

Figure 8: (a) TEM DF of a γ- γ' eutectic product (b) SADPs from the eutectic product. Bold angles are the measured total tilt angles while the unbold angles are the calculated angles. (c) Schematic Kikuchi map for the zones in (b).

Ojo, O.A. and M.C. Chaturvedi, On the role of liquated γ' precipitates in weld heat affected zone microfissuring of a nickel-based superalloy. Materials Science and Engineering a-Structural Materials Properties Microstructure and Processing, 403: 77-86, 2005.

Ola, O.T., O.A. Ojo, P. Wanjara, and M.C. Chaturvedi, *Enhanced resistance to weld cracking by strain-induced rapid solidification during linear friction welding*. Philosophical Magazine Letters, 91(2): 140-149, 2010.

Pepe, J.J. and W.F. Savage, *Effects of constitutional liquation in 18-Ni maraging steelweldments.*Welding Journal, 46(9): 411-422, 1967.

Prager, M. and C.S. Shira, *Welding of precipitation-hardening nickel-base alloys.* Welding Research Council -- Bulletin Series 128, p. 55, 1968.

Unfried, J., T.F. Hermenegildo and A.J. Ramirez, *Influence of Process Parameters in the TMAZ Microstructural Evolution of C-Mn Steels Friction Hydro-Pillar Welded Joints.* Trends in Welding Research, pp. 381-384, 2009.

Wang L., M. Preuss, P.J. Withers, G. Baxter, and P. Wilson, *Energy-input based finite-element process modeling of inertia welding.* Metallurgical and Materials Transactions B: Process Metallurgy and Materials Processing Science, 36(4): 513-523, 2005.